

RESEARCH

Open Access



Inhibition of the cardiac fibroblast-enriched histone methyltransferase Dot1L prevents cardiac fibrosis and cardiac dysfunction

Jie Xu[†], Jinghuan Wang[†], Fen Long, Wen Zhong, Haibi Su, Zhenghua Su and Xinhua Liu*

Abstract

Background: Cardiac fibrosis is characterized by excessive extracellular matrix deposition that contributes to compromised cardiac function and potentially heart failure. Disruptor of telomeric silencing 1-like (Dot1L) is the catalytic enzyme required for histone H3K79 methylation which has been demonstrated to play a role in transcriptional activation. However, the functions of Dot1L in the process of cardiac fibrosis still remain unknown.

Results: In the present study, we found that endogenous Dot1L is upregulated in cardiac fibroblasts (CFs) treated with angiotensin II (Ang II) or transforming growth factor (TGF)- β 1, along with elevated extracellular matrix (ECM) such as fibronectin, collagen I and III. Silencing or inhibiting Dot1L mitigated Ang II-induced myofibroblast generation and fibrogenesis. We identified the transcription factor-forkhead box O (FoxO) 3a as a novel substrate of Dot1L, the transcriptional activating mark H3K79me3 level on the promoter of FoxO3a was increase in activated-CFs, and inhibition of Dot1L markedly decreased FoxO3a transcription accompanied by a significant decrease in the expression of fibrogenic gene. Knockdown of FoxO3a could alleviate ECM deposition induced by Ang II, on the contrary, overexpression FoxO3a resulting in CFs activation. Consistently, in vivo Dot1L ablation rescued myocardial ischemia-induced cardiac fibrosis and improved cardiac function.

Conclusions: Our findings conclude that upregulation of Dot1L results in activation of the cardiac fibroblasts to promote profibrotic gene, eventually causes cardiac fibrosis. Pharmacological targeting for Dot1L might represent a promising therapeutic approach for the treatment of human cardiac fibrosis and other fibrotic diseases.

Keywords: Dot1L, Cardiac Fibrosis, Cardiac fibroblasts, Cardiac function, FoxO3a

Introduction

Myocardial fibrosis (that is, excessive deposition of scar tissue) comes with numerous forms of heart disease such as myocardial infarction (MI), cardiomyopathy [1], myocarditis [2], and infiltrative diseases [3], and the following heart failure is the leading cause of death in the world [4,

5]. Myocardial fibrosis manifests as excessive deposition of extracellular matrix (ECM), along with the synthesis and arrangement of series of ECM proteins disordering, significantly decreased cardiac output, which eventually contributes to the progression of heart failure. Despite substantial improvements in therapeutic strategies, there are few effective therapeutic approaches for suppressing the development of myocardial fibrosis. Thus, therapies and strategies to reduce myocardial fibrotic changes are extremely important in treating cardiovascular disease.

The tissue-resident cardiac fibroblast (CFs) is the predominant cell to mediate progressive cardiac fibrosis. Under pathological stimulation, they become activated

[†]Jie Xu and Jinghuan Wang contributed equally to this work

*Correspondence: liuxinhua@fudan.edu.cn

School of Pharmacy, Pharmacophenomics Laboratory, Human Phenome Institute, Fudan University, 825, Zhangheng Road, Pudong New District, Shanghai 201203, People's Republic of China



© The Author(s) 2022. **Open Access** This article is licensed under a Creative Commons Attribution 4.0 International License, which permits use, sharing, adaptation, distribution and reproduction in any medium or format, as long as you give appropriate credit to the original author(s) and the source, provide a link to the Creative Commons licence, and indicate if changes were made. The images or other third party material in this article are included in the article's Creative Commons licence, unless indicated otherwise in a credit line to the material. If material is not included in the article's Creative Commons licence and your intended use is not permitted by statutory regulation or exceeds the permitted use, you will need to obtain permission directly from the copyright holder. To view a copy of this licence, visit <http://creativecommons.org/licenses/by/4.0/>. The Creative Commons Public Domain Dedication waiver (<http://creativecommons.org/publicdomain/zero/1.0/>) applies to the data made available in this article, unless otherwise stated in a credit line to the data.

and then differentiated into the myofibroblast, which is known as fibroblast-to-myofibroblast transition (FMT) [6, 7]. Numerous studies suggested that levels of circulating hormones such as angiotensin II (Ang II) and fibrogenic cytokines transforming growth factor are contributed to the activation of fibroblasts [8, 9]. The myofibroblasts are the most important effector cells in the process of myocardial fibrosis [10] and also responsible for secreting numerous cytokines, growth factors, and ECM that eventually resulted in cardiac fibrosis [11]. Thus, inhibition of myofibroblast conversion or their activity would be an attractive therapeutic strategy in adult fibrotic disease states, including heart failure [12].

In recent years, the breakout of epigenetics gradually penetrates into a variety of biological system [13]. Multiple epigenetic mechanisms are highly interdependent and closely associated with gene expression, including histone modifications, DNA methylation and regulatory noncoding RNAs [14]. Large numbers of transcription factors and signal transduction molecules are dynamic regulated by these epigenetic mechanisms through chromatin remodeling or other modifications on gene level [15]. Emerging data suggest that these epigenetic modifications also impact on the development of cardiac fibrosis [16, 17]. Dot1L (disruptor of telomeric silencing 1-like) is the only known H3K79 methyltransferase [18], and H3K79 methylation is mainly considered transcriptional activating when highly abundant. Dot1L was found to play an essential role in transcriptional elongation, DNA repair and cell cycle regulation [19, 20], making it an attractive therapeutic target for acute leukemia [21]. However, the functional role of Dot1L in the induction of cardiac fibrosis has still been vague.

Therefore, this study first provided insight into the functional role and mechanisms of Dot1L in cardiac fibrosis. Using combinative *in vitro* and *in vivo* studies, we demonstrated that Dot1L is a critical component of pro-fibrotic signaling in the heart, and determined the therapeutic potential of specific inhibitor EPZ5676 in cardiac fibrosis of post-MI. Furthermore, transcription factor forkhead box O (FoxO) 3a was identified as a specific and effective target for Dot1L in activation of the cardiac fibroblasts, and we concluded that inhibition of the cardiac fibroblast-enriched histone methyltransferase Dot1L alleviates cardiac fibrosis and cardiac dysfunction.

Results

Dot1L is upregulated in TGF- β 1-induced adult rat CFs and fibrotic mouse hearts

TGF- β 1 can drive myofibroblast activation, as Fig. 1A showed, markers of fibrosis such as Collagen I (Col 1), fibronectin (FN) and connective tissue growth factor (CTGF) were abundantly expressed in activated CFs

by different concentration of TGF- β 1, as well as Dot1L expression. Besides, an increased expression of Dot1L was presented at different time after stimulation with TGF- β 1, along with expressions of Col 1, Col 3, FN and CTGF (Fig. 1B). Furthermore, immunofluorescence double staining showed that the expressions of Dot1L and CTGF were increased in TGF- β 1-induced CFs (Fig. 1C). Thus, 5 ng/mL TGF- β 1 was applied to activate adult rat CFs for 48 h in subsequent experiments.

To further explore whether Dot1L level was increased in response to cardiac fibrosis *in vivo*, cardiac fibrosis post-MI was induced by permanent ligation of the left ascending artery (LAD) in mice. Consistently, after 2 weeks of LAD ligation, MI model mice exhibited obvious upregulation of Dot1L in comparison with sham mice, along with notably increase of protein levels of the fibrosis markers Col 3 and CTGF (Fig. 1). These results suggest that Dot1L is upregulated during MI and may participate in cardiac fibrosis.

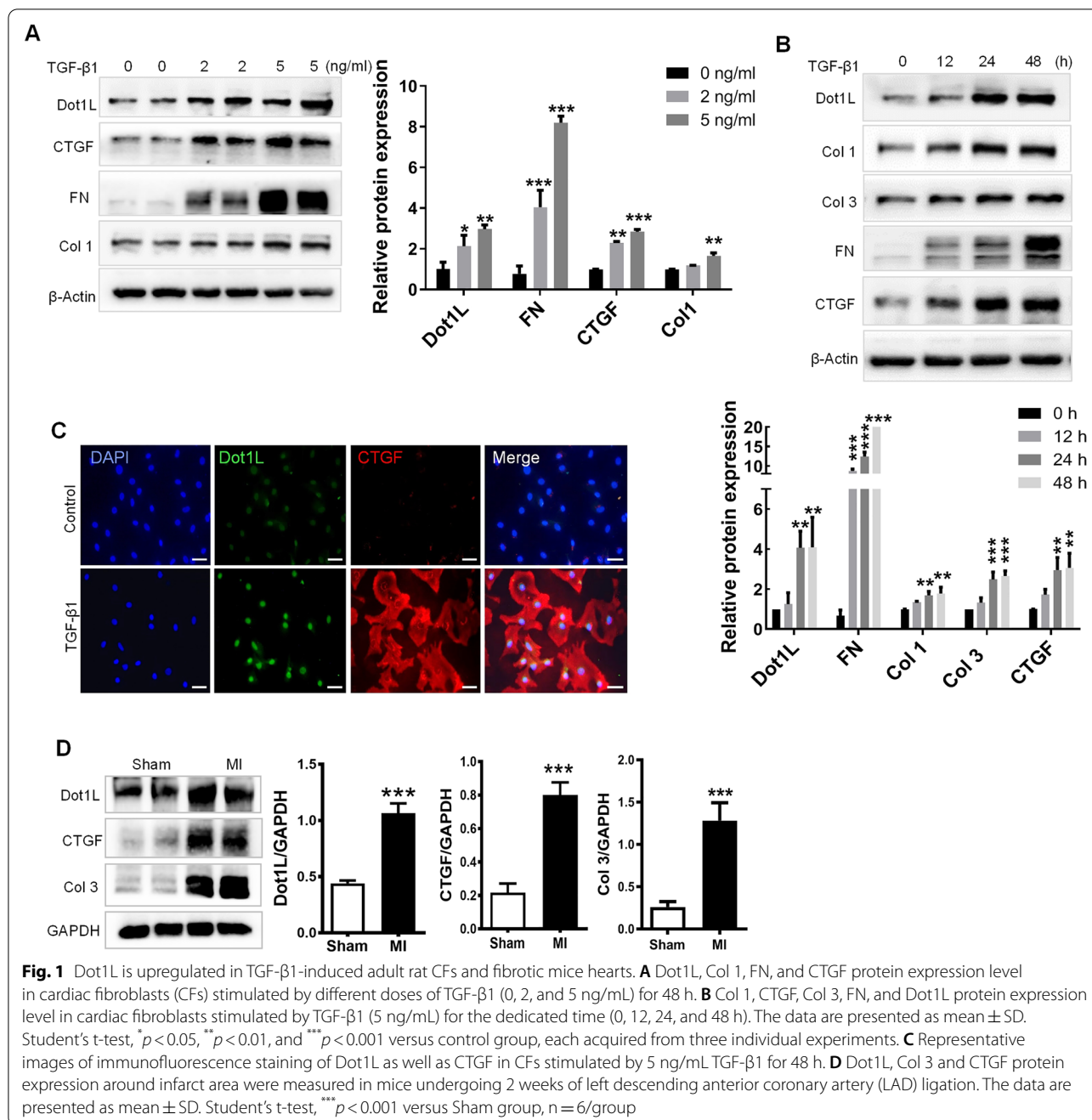
Dot1L ablation attenuates TGF- β 1-induced ECM deposition in adult rat CFs

We next explored the direct link between Dot1L upregulation and fibrosis in cultured adult rat CFs. Firstly, to verify whether silencing Dot1L would prevent fibrosis in adult rat CFs, we used siRNA to knock down Dot1L expression (Fig. 2A). Consistently, silencing Dot1L prevented the TGF- β 1-induced the increase in the expression of fibrosis-related markers, such as FN, Col 3, and matrix metalloproteinase (MMP) 9 (Fig. 2A). In addition, immunofluorescence double staining also confirmed silencing Dot1L decreased CTGF expression (Fig. 2B).

Small molecule Dot1L inhibitor such as EPZ5676 can inhibit methylation effect of Dot1L on H3K79, as Dot1L is the only methyltransferase acting on histone H3K79. We found that EPZ5676 co-treatment could decrease H3K79me3 expression and the synthesis of TGF- β 1-induced CTGF, FN, Col 1, and MMP9 to below baseline levels (Fig. 2C). Immunofluorescence staining also confirmed EPZ5676 treatment exhibited decreased CTGF and Col 1 expressions upon TGF- β 1 (Fig. 2D). These results demonstrate that knocking down or inhibiting Dot1L could suppress TGF- β 1-induced ECM deposition *in vitro*.

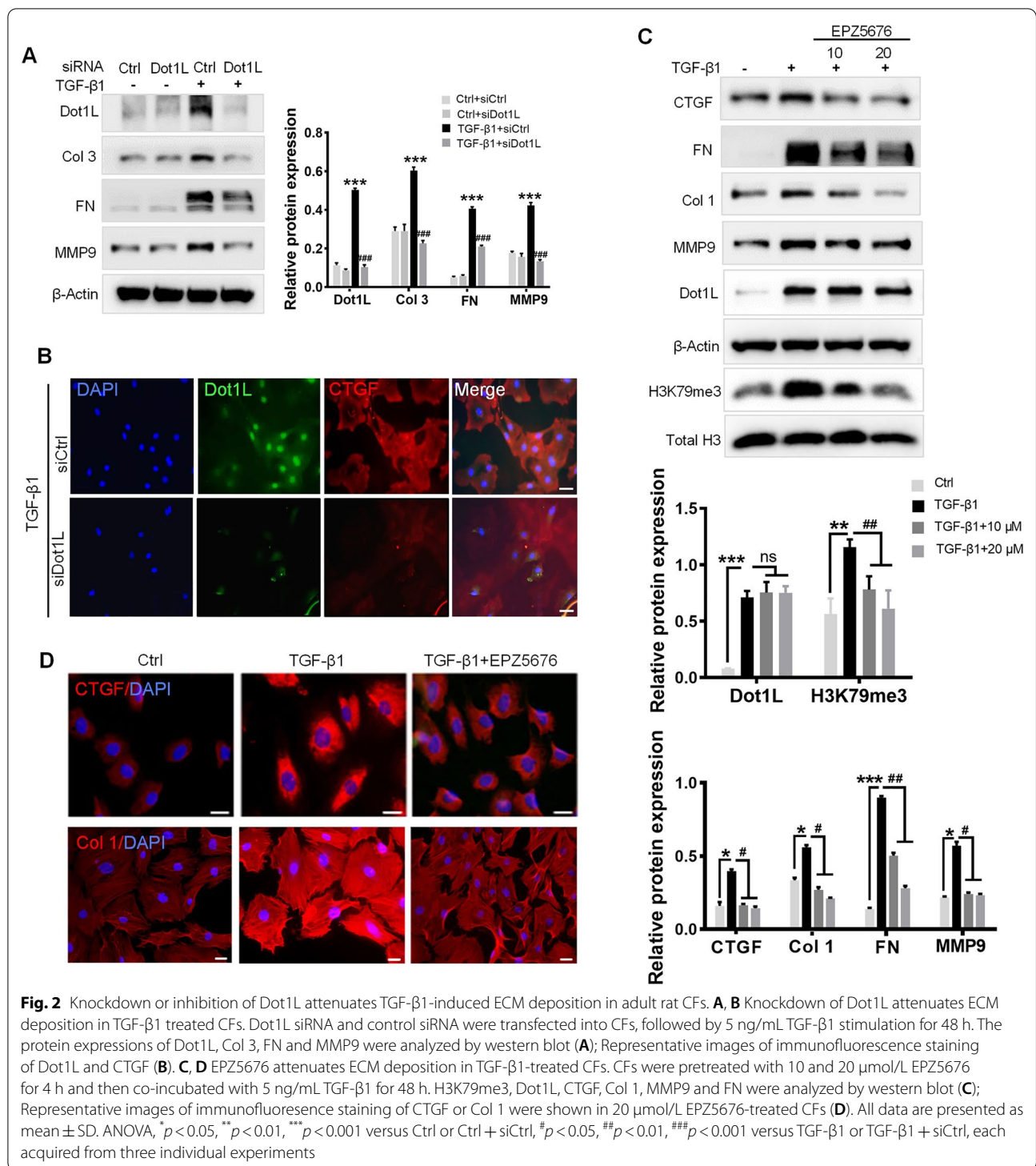
Dot1L ablation attenuates Ang II-induced fibrosis in neonatal rat CFs (NRCFs)

Ang II also plays an important role in myocardial remodeling after MI [22, 23], we applied Ang II-induced NRCFs and analyzed the relative levels of Dot1L and collagen synthesis. We performed western blot to examine Dot1L expression and markers of fibrosis, which was up-regulated by Ang II (Fig. 3A). In



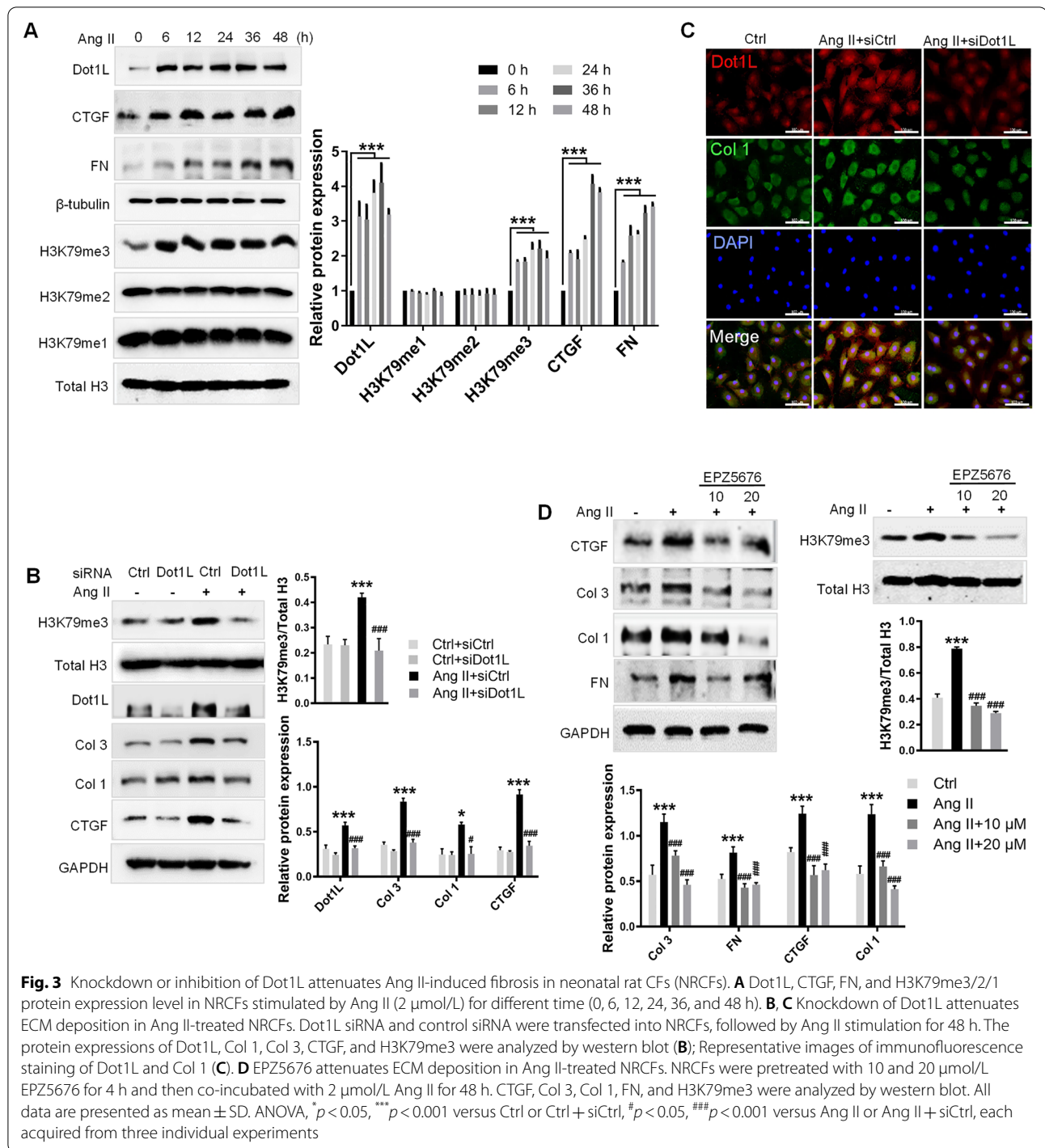
addition to the dynamic change in Dot1L expression, we also observed increased deposition of H3K79me3 with no obvious change in H3K79me2/me1 expression, providing an assumption that Dot1L played an important role in cardiac fibrosis via its tri-methylation on H3K79 (Fig. 3A). Furthermore, we treated NRCFs with Dot1L siRNA to determine the effect of Dot1L on Ang II-induced fibrosis, and found silencing Dot1L significantly decreased the expression of CTGE, Col 1 and Col

3 in NRCFs (Fig. 3B). Consistent with a reduced expression of Dot1L expression, silencing Dot1L exhibited a decrease in H3K79me3 abundance relative to total histone H3 levels (Fig. 3B). Similarly, immunofluorescence assay further confirmed that Ang II enhanced the co-expression between Dot1L and Col 1, while silencing of Dot1L decreased Col 1 expression (Fig. 3C). Pretreating the Ang II-stimulated fibroblasts with EPZ5676 suppressed fibrosis-related markers, such as FN, CTGE,



Col 1, and Col 3 expression (Fig. 3D). Consistently, EPZ5676 exhibited a decrease in H3K79me3 abundance relative to total histone H3 levels in activated neonatal rat CFs (Fig. 3D). Together, we had similar findings in Ang II-stimulated CFs from neonatal rat, where Dot1L

levels were markedly increased, and ablation of Dot1L inhibited fibroblast activation. The change in Dot1L ablation was consistent with TGF-β1-stimulated CFs from adult rat. These observations support that Dot1L contributes to cardiac fibrosis.



Inhibiting Dot1L prevents cardiac fibrosis and dysfunction during MI

To explore the role of Dot1L during cardiac fibrosis post LAD-induced MI, we conducted a LAD procedure followed by intraperitoneal injection of EPZ5676 (20 mg/kg/day) from 1 day after LAD for 2 weeks. To assess

cardiac function, we performed echocardiographic on day 14 post-LAD. Echocardiographic showed that comparing with the sham group, LAD treatment worsened both left ventricular (LV) function and structure, as indicated by expanded LV dimension and weakened LV systolic function. EPZ5676 treatment protected against

the LAD-induced cardiac dysfunction (Fig. 4A). We next investigated whether EPZ5676 treatment of mice for 2 weeks could ameliorate the LAD-induced cardiac fibrosis, as deposition of fibrotic tissue was main cause of unfavourable heart remodeling in MI. Therefore, we evaluated the heart fibrosis degree by Masson's trichrome staining, obviously, EPZ5676 treatment effectively alleviated cardiac fibrosis reflected with marked reduction in fibrosis area and degree (Fig. 4B). After a 2-week treatment, EPZ5676 significantly alleviated the protein levels

of the cardiac fibrosis markers Col 1, CTGF, MMP9 and FN (Fig. 4C). Consistently, Col 3 expression were notably increased in MI mice compared with all other groups by immunohistochemistry (IHC) analysis (Fig. 4D). Furthermore, immunofluorescence analysis of sections of hearts further revealed that MMP9 protein expression was downregulated while treated with EPZ5676 (Fig. 4E). Compared to clear transverse striations in sham group shown by H&E staining, the myocardial cells in mice after LAD ligation were irregular shape and the

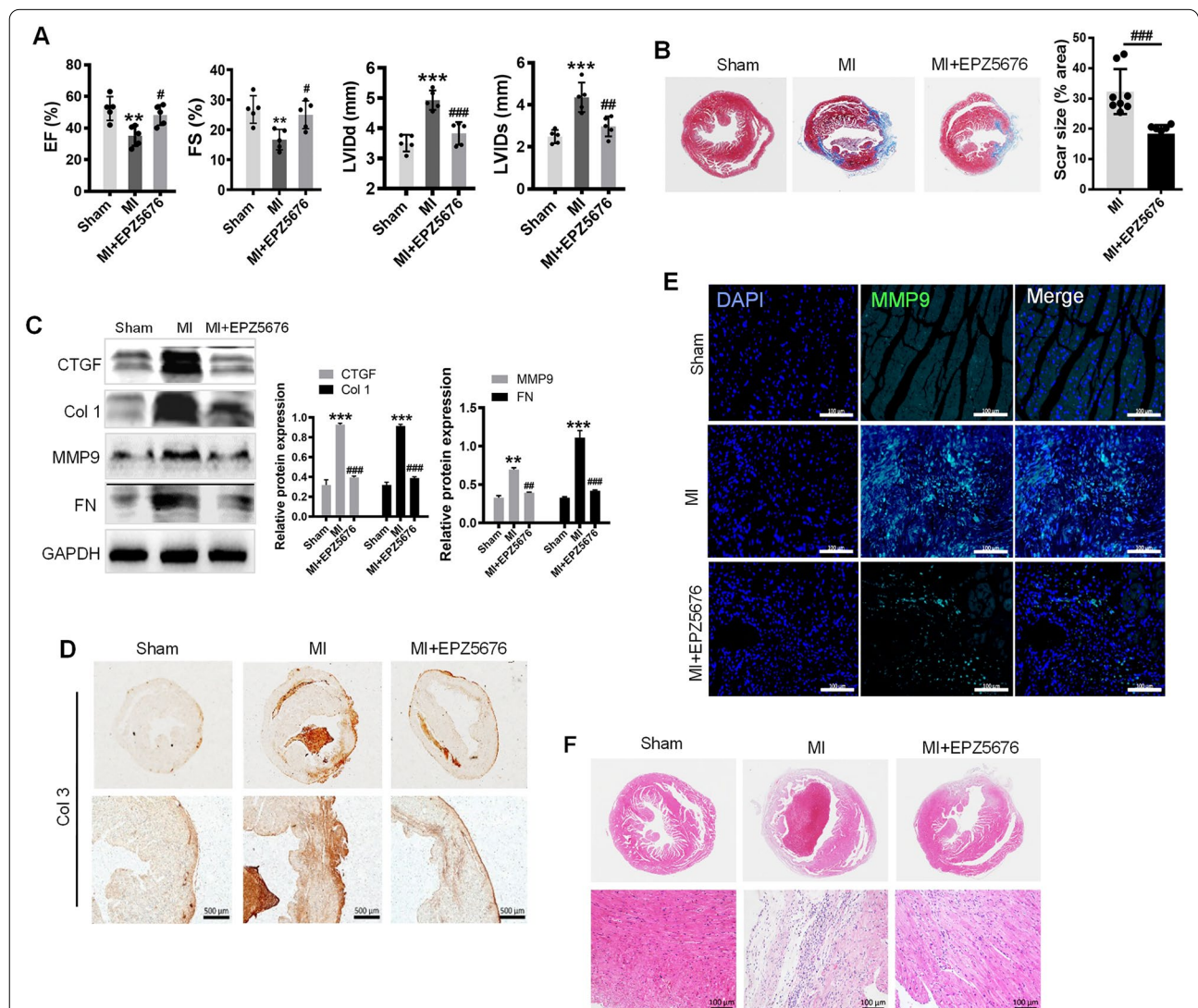


Fig. 4 Inhibiting Dot1L prevents cardiac fibrosis and improves cardiac function during MI. EPZ5676 at a dose of 20 mg/kg/day was administered to mice undergoing LAD ligation by intraperitoneal injection for 14 days. **A** The echocardiographic parameters at the 14th day post-MI were statistically analyzed and shown in the graphs, including EF%, FS%, LVIDs and LVIDd. **B** Masson's trichrome staining of cross sections of whole heart and Scar size were analyzed. **C** Western blot was performed to analyze the expression of CTGF, Col 1, MMP9 and FN. **D** Representative images of immunohistochemistry staining of Col 3. **E** Representative images of immunofluorescence staining of MMP9. **F** Representative images of H&E staining at magnification of 50 X and 200 X respectively. Data are represented as means ± SD. ANOVA, ** $p < 0.01$, *** $p < 0.001$ versus Sham group, # $p < 0.05$, ## $p < 0.01$, ### $p < 0.001$ versus MI, $n = 5-8$ /per group

transverse striations were blurry and broken. Whereas, in EPZ5676-treated mice after LAD ligation, myocardial cells were neatly arranged with decreased degree of fibroplasias (Fig. 4F). Taken together, the results confirm the pathogenesis of cardiac fibrosis in MI mice and inhibiting Dot1L attenuates the pathological remodeling and improves cardiac function.

Knocking down Dot1L alleviates cardiac fibrosis and improves cardiac function

To elucidate the important role of Dot1L in cardiac fibrosis after injury, we generated a lentivirus carrying Dot1L

shRNA. After the LAD ligation, knockdown of cardiac Dot1L was successfully determined by injection of lentivirus carrying Dot1L shRNA into myocardium at several positions surrounding the infarct border zone. Firstly, we verified the decrease of Dot1L protein expression in heart (Fig. 5A). In accordance with the findings above, the concomitant expressions of CTGF, FN, MMP9, and Col 1 were dramatically increased in the MI mice compared with the sham group. However, MI mice injected with Dot1L shRNA showed great reduction in those fibrosis markers in comparison with the MI mice (Fig. 5A), illustrating a pivotal role of Dot1L in cardiac myofibroblast

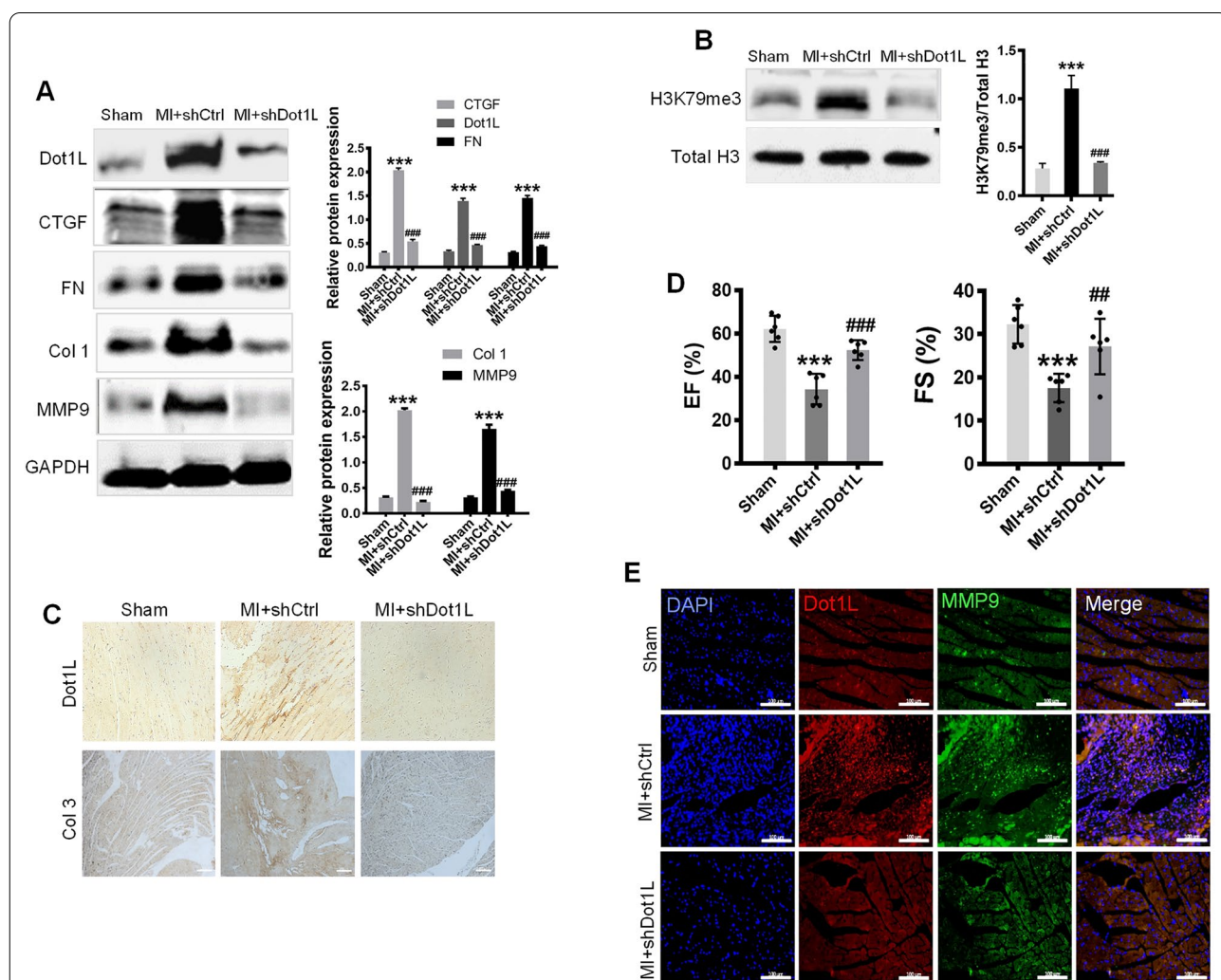


Fig. 5 Knockdown of Dot1L alleviates cardiac fibrosis and improves cardiac function during MI. Lentivirus carrying Dot1L shRNA (shDot1L) or Control shRNA (shCtrl) was injected into myocardium of mice undergoing LAD ligation for 14 days to specially knock down the cardiac Dot1L. **A** The expressions of Dot1L, CTGF, FN, Col 1, and MMP9 in MI mice were analyzed by western blot. **B** The level of H3K79me3 was analyzed by western blot. **C** Representative images of immunohistochemistry staining of Dot1L and Col 3 of cross sections of whole heart from MI mice. **D** Cardiac functions were measured by echocardiography and EF%, FS% were also statistically analyzed. **E** Representative images of immunofluorescence double staining of Dot1L and MMP9 of cross sections of whole heart. All data are represented as means ± SD. ANOVA, ****p* < 0.001 versus Sham group, ##*p* < 0.01, ###*p* < 0.001 versus MI treated with shCtrl, n = 6/per group

activation in vivo. Consistent with a reduced expression of Dot1L, H3K79me3 abundance relative to total histone H3 level exhibited a decrease (Fig. 5B). IHC further confirmed the knockdown of Dot1L attenuated the expressions of Dot1L and Col 3 (Fig. 5C). To evaluate whether cardiac function was influenced by knockdown of Dot1L, echocardiograph was performed. MI mice injected with Dot1L shRNA exhibited remarkable improvement in ejection fraction (EF) and fractional shortening (FS) compared with MI mice (Fig. 5D). Besides, immunofluorescence was performed to check synchronous change between Dot1L and MMP9, which turned out to be consistent with the western blot results (Fig. 5E). In summary, the results suggest that knockdown of Dot1L alleviates cardiac fibrosis and ameliorates cardiac function after MI.

Dot1L^{+/-} mice present the cardio-protective effect during MI

Next, we generated mice with a whole-body knocking down to determine Dot1L functions in cardiac fibrosis. Dot1L heterozygotes (Dot1L^{+/-}) were studied because homozygotes are not viable. The relative decrease of Dot1L protein level in heart was verified (Fig. 6A). Consistent with a reduced expression of Dot1L, Dot1L^{+/-} mice exhibited a decrease in H3K79me3 abundance relative to total histone H3 levels (Fig. 6A). Dot1L[±] and WT mice were performed with LAD ligation. After 2 weeks, post-infarct ventricular remodeling in WT and Dot1L^{+/-} mice was assessed with echocardiography. WT and Dot1L[±] hearts had comparable chamber dimensions and ventricular function before LAD ligation, but after 2 weeks post-MI, Dot1L[±] animals had an improved LV function as reflected by increased EF and FS (Fig. 6B). Then, Masson trichrome staining and Sirius red staining were used to determine the extent of cardiac fibrosis, showing that Dot1L[±] mice with LAD ligation exhibited relieved cardiac fibrosis compared with WT mice with LAD ligation (Fig. 6C, D). As expected, Col 3, MMP9, CTGF, and α -smooth muscle actin (α -SMA) expressions in Dot1L[±] mice after ligation were significant reduced compared with WT mice receiving ligation, where there was nearly no comparable change between Dot1L[±] mice and WT mice before ligation (Fig. 6E). Further, immunofluorescence double staining analysis of sections of hearts revealed that Dot1L[±] mice had a decreased CTGF protein expression (Fig. 6F). In a word, these findings indicate Dot1L regulated cardiac remodeling after injury.

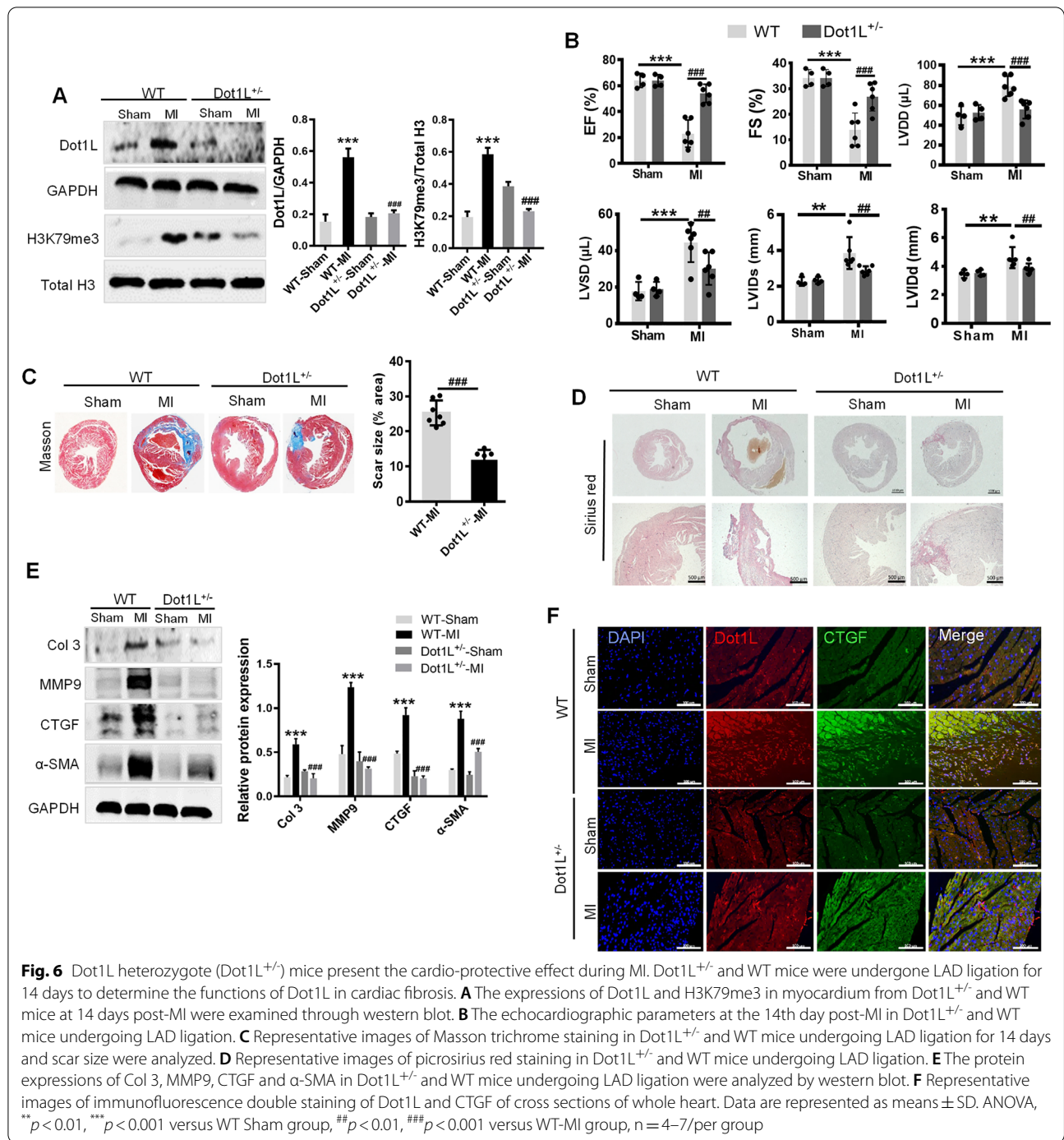
Dot1L expression is mediated by p-Smad2/3 in Ang II-induced CFs

The Smad2/3 signaling pathway was activated in cardiac fibrosis, we examined whether Smad2/3 activation up-regulated Dot1L expression. We found that Ang II stimulated phosphorylation of Smad2/3 in CFs (Additional file1: Fig S1A). To further validate the Smad2/3 regulatory role on Dot1L, Smad2/3 was knocked down by siRNA. The result showed that depletion of Smad2/3 led to a decrease in Smad2/3 and Dot1L protein level, along with reduced fibrosis markers such as CTGF and Col 3 (Additional file1: Fig S1B). Meanwhile, Sis, an inhibitor of Smad3, was also proved to decrease Dot1L and fibrosis markers expression in a dose-dependent manner, showing that reduction of Smad2/3 activity can reverse increased expression of Dot1L (Additional file1: Fig S1C). These results suggest that upregulation of Dot1L in Ang II-induced cells is mediated by Smad3-dependent mechanism.

Dot1L directly binding to the promoter regions of FoxO3a activates CFs

We next investigated the underlying mechanism by which Dot1L promotes myocardial fibrosis. FoxO3a plays an important role in regulating several essential cellular functions. We found that an increased FoxO3a protein level by Ang II at time-dependent manner in CFs, while p-FoxO3a expressions were reduced (Fig. 7A). Meanwhile, we strikingly found that silencing FoxO3a expression exerted anti-fibrotic effect (Fig. 7B). Besides, immunofluorescence was performed to check synchronous change between FoxO3a and CTGF, which turned out to be consistent with the western blot results (Fig. 7C). Further, silencing or inhibiting Dot1L led to a decrease in FoxO3a protein level in Ang II-induced CFs (Fig. 7D). As Dot1L is the only methyltransferase targeting H3K79, the increase of H3K79me3 levels near the promoter of FoxO3a was validated by ChIP-PCR at Ang II-treated CFs (Fig. 7E). RT-qPCR validated the increased FoxO3a mRNA abundance upon Ang II treatment, instead, inhibiting Dot1L decreased FoxO3a transcription level (Fig. 7F). These data suggest that Dot1L transcriptionally activates FoxO3a via its H3K79 methylation dependent function.

Next, we sought to determine whether FoxO3a results in ECM deposition, we examined fibrosis marker expression through transfecting CFs cells with pCMV-FoxO3a. We observed that overexpression of FoxO3a (FoxO3a OE) in CFs could significantly cause consistently fibrosis marker expression such as CTGF, Col 1, Col 3, MMP9, and FN (Fig. 7G). Immunofluorescence analysis further revealed that overexpression of



FoxO3a resulted in increased CTGF protein expression (Fig. 7H). These data suggest that FoxO3a positively regulates ECM deposition in CFs.

Discussion

Excess activation and proliferation of CFs after MI greatly contribute to adverse cardiac remodeling and increase the risk of chronic heart failure. Dot1L mediated-methylation of histone H3K79 is symbolically presented in many actively transcribed genes [24]. In this study, we demonstrated that Dot1L could be a novel

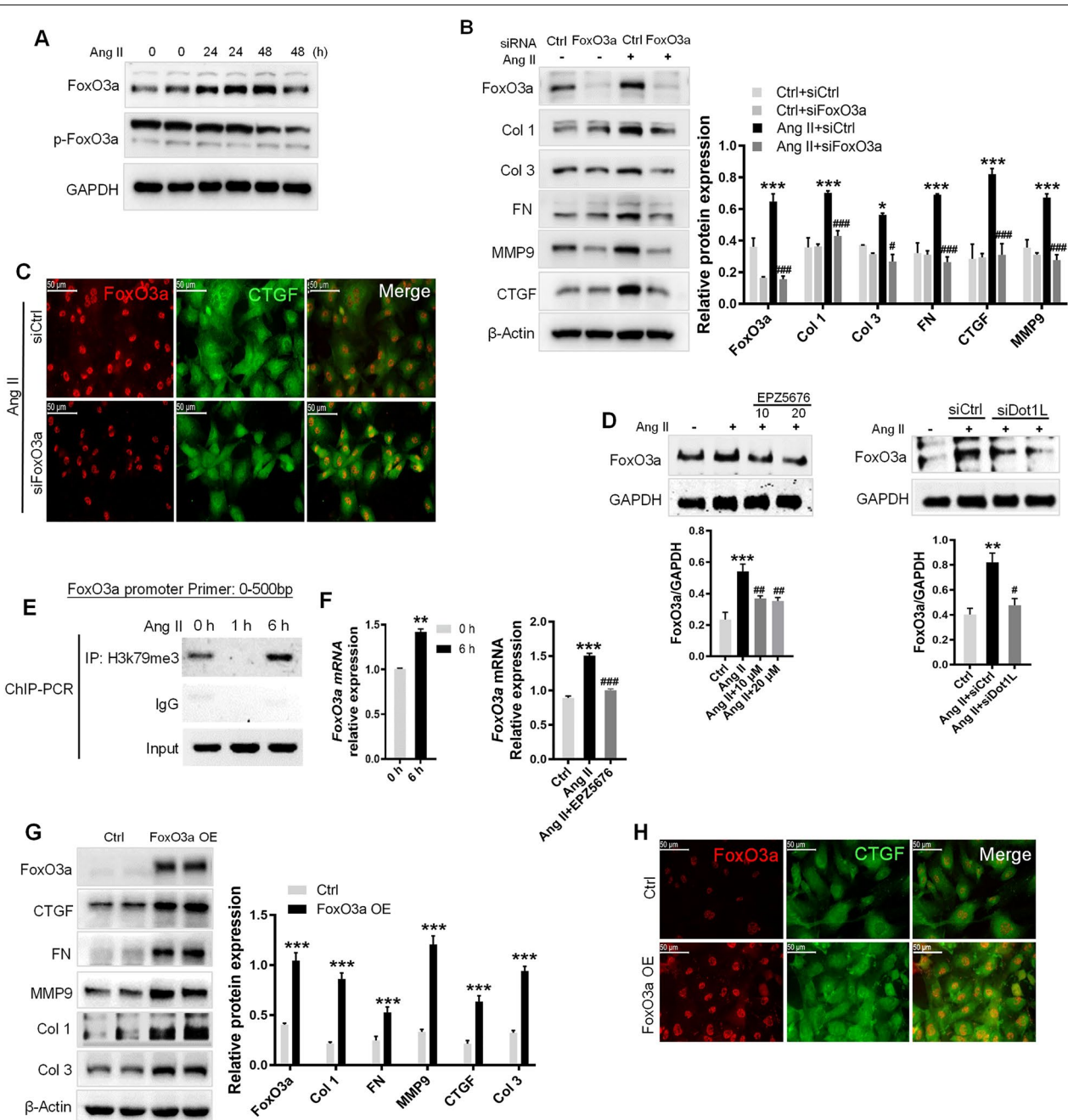


Fig. 7 Dot1L directly binding to the promoter regions of FoxO3a promotes ECM deposition. **A** FoxO3a is upregulated in NRCFs treated with 2 μmol/L Ang II for 24 and 48 h. FoxO3a and its phosphorylation form were analyzed by western blot. **B, C** Knockdown of FoxO3a attenuates ECM deposition in Ang II-treated NRCFs. FoxO3a siRNA and control siRNA were transfected into NRCFs, followed by Ang II stimulation for 48 h. The protein expressions of FoxO3a, Col 1, Col 3, FN, MMP9 and CTGF were analyzed by western blot (B); Representative images of immunofluorescence staining of FoxO3a and CTGF in Ang II-stimulated NRCF (C). **D** NRCFs were pretreated with EPZ5676 (10, 20 μmol/L) for 4 h or transfected with siDot1L for 12 h, then incubated with 2 μmol/L Ang II for 48 h. FoxO3a was analyzed by western blot. **E** ChIP-PCR showing H3K79me3 gain in promoter of FoxO3a in Ang II-treated NRCFs. NRCFs treated with Ang II for 1 and 6 h were used for ChIP assay with antibody against H3K79me3. **F** mRNA level of FoxO3a was quantified by qRT-PCR after inhibition of Dot1L with EPZ5676. Above all data are represented as means ± SD. ANOVA, **p* < 0.05, ***p* < 0.01, ****p* < 0.001 versus Ctrl or Ctrl + siCtrl, #*p* < 0.05, ##*p* < 0.01, ###*p* < 0.001 versus Ang II or Ang II + siCtrl, each acquired from three individual experiments. **G, H** Overexpression of FoxO3a promotes fibrosis response in NRCFs. NRCFs were transfected with lentivirus containing FoxO3a overexpression plasmid for 24 h, and then cultured with completed medium for 48 h. The protein expressions of FoxO3a, CTGF, FN, MMP9, Col 1 and Col 3 were analyzed by western blot. Data are represented as means ± SD. Student's t-test, ****p* < 0.001 versus Ctrl, each acquired from three individual experiments (G); immunofluorescence double staining of FoxO3a and CTGF (H)

myofibroblasts activator, which upregulation in a mouse model of MI is an accomplice in myocardial fibrosis and consequent heart failure via FoxO3a-induced fibroblast activation and differentiation into collagen-producing myofibroblasts. In addition, we have also shown that the knockdown Dot1L or administration of specific inhibitor decreased myocardial fibrosis and improved heart function, and it ameliorated ventricular remodeling in mouse MI model. Thus, our study identifies Dot1L as a new player involved in myocardial fibrosis after MI injury.

Since the discovery of Dot1L as histone methyltransferase targeting on histone H3K79, great progress has been made in uncovering the role of this methylation modification in different physiological and pathological conditions, especially in the MLL-rearranged leukemias. Previous researches have demonstrated that a variety of epigenetic mechanisms was widely involved in cardiovascular diseases (CVDs) [25], as an important branch of epigenetic pathway, the role of Dot1L-mediated H3K79 methylation in CVDs is gradually revealed. Studies have shown that cardiac-specific conditional knockout of Dot1L in mice led to cardiac dilatation and postnatal lethality, confirmed that Dot1L activated key cardiac genes in cardiomyocyte differentiation and maturation by catalyzing different degrees of methylation on H3K79 [26, 27], indicating the important regulation of Dot1L in heart development. It's also demonstrated that Dot1L was involved in atherosclerosis development through NF- κ B pathway [28]. Our study revealed that Dot1L was a critical component of pro-fibrotic signaling after MI. Almost simultaneously, another work verified that Dot1L promoted the expression of spleen tyrosine kinase by increasing the H3K79me2 modification on its promoter and activated TGF- β 1/Smad3-mediated myocardial injury [29]. Taken together, current researches have brought insight into the relevance of Dot1L to CVDs. There is a reasonable prospect that Dot1L would have enormous therapeutic potential in heart diseases coupled with in-depth knowledge of underlying mechanism of CVDs.

Our work also provided insights into the mechanism by which Dot1L inhibition affords cardioprotection following acute insults in MI model induced by LAD. In line with the previous reports, MI badly damages heart function [30, 31], which presents as attenuated cardiac contractile function along with significant structural remodeling, a significant decrease in ejection fraction and LV volume at both diastole and systole, indicating a progressive pathological remodeling of the myocardium in response to the MI insult. Further, we provided evidence that in mice with either systolic or diastolic dysfunction, higher level of Dot1L showed high commonality in severe

cardiac interstitial fibrosis. Thus, efforts were made to test our hypothesis that upregulated cardiac Dot1L may mediate fibrosis and contribute to cardiac dysfunction. Fortunately, the following study illustrated that blockade of Dot1L in MI-induced mice cardiac remodeling alleviated fibrotic ECM deposition, and improved cardiac function. EPZ5676, a Dot1L specific inhibitor, treatment for 2 weeks post-MI alleviated cardiac interstitial fibrosis and the MI-induced increase in LV mass. Further, EF at 2 weeks after MI under treatment with EPZ5676 was better preserved than not, and same improvement on infarct scar thinning and infarct expansion were obtained. The latter is associated with decreased LV systolic function and increased infarct rupture at the infarct border zone [32]. In other words, treatment with EPZ5676 ameliorated the damage to LV systolic function and provided protection from infarct rupture, all of which contributed to better post-MI cardiac function. Meanwhile, Dot1L^{+/-} mice or knocking down of Dot1L by shRNA via a lentiviral vector limited cardiac fibrosis along with ameliorative cardiac function. The improvement of LV compliance and cardiac function could attribute to decreased LV fibrosis and cardiac remodeling.

Under the pathologically myocardial injury, fibroblasts activate and differentiate into myofibroblast, which display increased ability of proliferation, migration, and collagen production [33, 34]. Following an acute myocardial injury, CFs within the connective tissue convert to their activated form, which secrete elevated levels of ECM proteins to promote a profibrotic environment [35]. Cardiac fibrosis provokes a series of pathological changes including chamber dilatation, cardiomyocytes hypertrophy and apoptosis, and culminate in congestive heart failure [36]. Multiple signaling pathways are orchestrated in the cardiac fibrotic response. Among them, Ang II and TGF- β , have been demonstrated to be implicated in activation of CFs, fibroblast-to-myofibroblast transition and ECM deposition during the process of fibrosis [37]. We found that stimulation of normal fibroblasts with recombinant TGF- β or Ang II not only led to transformation into fibroblast phenotype, but also upregulated Dot1L expression. The upregulation of Dot1L in fibroblasts is thus consistent with fibrosis response. TGF- β or Ang II can induce serine phosphorylation of Smad2/3 and translocate into the nucleus to promote specific gene transcription [38]. We found Dot1L expression was mediated by Smad2/3 signaling and fibroblast activation was under the control of Dot1L. Blockade of Dot1L could significantly inhibit collagen deposition and myofibroblast differentiation.

Previous researches have established that Forkhead box O (FoxO) proteins, a transcription factor family, play a vital role in the regulation of cardiac fibroblast

proliferation and differentiation [39]. Many proteins associated with fibrosis, such as Col 1, CTGF, and α -SMA can be used as biomarker for CFs differentiation. In skin fibroblasts, ultraviolet light increases Col 1 expression via FoxO1 activation, whereas FoxO1 down-regulation eliminates this effect [40]. Furthermore, FoxO1 is necessary for CTGF expression in HUVEC [41] or primary keratinocytes [42]. Our results showed that FoxO3a overexpression promoted Col 1, Col 3, FN, and CTGF expression. In corresponding, knock-down of FoxO3a inhibited the effects of Ang II on differentiation shown by multiply markers, indicating that FoxO3a contributing to the CFs differentiation induced by Ang II. Importantly, FoxO3a signaling pathway was mediated by Dot1L in Ang II-induced CFs, by a mechanism related to FoxO3a transcription regulation. Dot1L initiated H3K79me3 enrichment in the promoter of FoxO3a and consequently activated its transcription, consistent with Dot1L's methyltransferase activity on H3K79. Taken together, results from this study suggest that Dot1L transcription regulates FoxO3a expression, which is crucial to the process of Ang II-induced CFs activation.

Conclusions

In this study, we provided evidence that increased levels of Dot1L contributes to MI-induced myocardial fibrosis and dysfunction in mice. Additionally, we proved that in cardiac fibroblasts, the expression of Dot1L is upregulated under the stimulation of Ang II, cascading the activation of following profibrotic signaling. Thus, we proposed that myocardial Ang II signaling leads to upregulation of the Dot1L to facilitate differentiation from cardiac fibroblasts into collagen-producing myofibroblasts, which is vital to development of myocardial fibrosis and heart failure. Therefore, Dot1L may be a potential target for improving heart function following an ischemic insult.

Materials and methods

Reagents and antibodies

Transforming growth factor- β 1 was obtained from ProteinTech (Proteintech, USA). Angiotensin II was obtained from Meilunbio (Meilun Biotechnology, Dalian, China). EPZ5676 (Dot1L inhibitor) was purchased from Selleckchem (Selleck, USA). Antibody against Dot1L (sc-390879) and CTGF (sc-365970) were obtained from Santa Cruz Biotechnology (Santa Cruz, CA); total H3 (4499), Smad2/3 (8685S) and p-Smad2/3 (8828S) were purchased

from Cell Signaling Technology (Danvers, MA, USA). Antibody against CTGF (ab6992), H3K79me3 (ab2621), H3K79me1 (ab177183) and p-FoxO3a (ab154786) were purchased from Abcam; Col 3 (GB11023); MMP9 (GB12321-1), and α -SMA (GB13044) were purchased from Servicebio (Wuhan, China). Antibody against Dot1L (A11285), fibronectin (A7488), Col 1 (A5786), H3K79me2 (A2368) were purchased from ABclonal (Wuhan, China); FoxO3a (66,428-1-Ig) and GAPDH (60,004-1-Ig) were obtained from Proteintech (USA).

Culture of primary adult and neonatal rat cardiac fibroblasts (CFs)

Adult Sprague–Dawley rats (130–150 g) and neonatal rat (1–3 days) were applied in the study. Briefly, the extracted ventricle from adult mice or neonatal rats was washed with cold PBS buffer and finely cut into pieces. Then the heart was digested in 0.25% trypsin with EDTA for 5 min at 37 °C with gently stirring all the time, which was repeated several times until the tissues disappeared. All digestive harvest was collected and centrifuged at 1000 rpm for 3 min. The cells were resuspended and plated for 2 h. Adherent cells were cardiac fibroblasts and cultured in DMEM completed medium (containing 10% fetal bovine serum, 1% penicillin and streptomycin), incubating at 37 °C in a humidified incubator with 5% CO₂. CFs with passages between 1 and 3 were used for all studies.

Western blot

The total protein extracted from cells or myocardial tissues using proper lysis solution were separated by SDS-PAGE, after which it was transferred to nitrocellulose membranes. Blocking in 5% skimmed milk to eliminate non-specific binding, then the membranes were incubated with appropriate primary antibodies overnight at 4 °C, followed by incubation with the speciesappropriate horseradish peroxidase (HRP)-labeled secondary antibody (Jackson ImmunoResearch Inc., USA). Protein-specific signals were detected using a Bio-Rad Imager (Bio-Rad, Hercules, CA, USA), and the relative expression levels were quantified by Alpha Imager (Alpha Innotech Corp, San Leandro, CA).

Real time quantitative polymerase chain reaction (RT-qPCR)

After lysing with TRIzol Reagent (TaKaRa Biotechnology, Dalian, China), the total RNA of CFs was prepared by the general Trizol extraction protocol. Total RNA of each sample was reversely transcribed into cDNA and amplified using a PrimeScript 1st Strand cDNA

Synthesis Kit (Takara) according to the manufacturer's directions. Utilizing RT-qPCR, the fluorescence intensity was determined by iCycler iQ system (Bio-Rad, Hercules, CA, USA) for semi-qualification of FoxO3a expression level, with the housekeeping gene GAPDH used as control. Primer sequences were listed below: FoxO3a: 5'-TCCTGGCGGGCTTATGCAG-3', 5'-GACATCATTGGGTCTGTTGCG-3'. GAPDH: 5'-TTCAACGGCACAGTCAAGG-3', 5'-CGGCATGTCAGATCCACAA-3'.

Construction of FoxO3a overexpression plasmid

The full-length coding sequence of FoxO3a was obtained from UCSC Genome Browser. The primers and the restriction enzyme cutting site towards FoxO3a were get from Primer-BLAST of NCBI and Webcutter 2.0, respectively. Using the cDNA of rat genome as template, the target sequence was amplified by Q5 high-fidelity enzyme. Then, the product was cut and connected to lentivirus vector using corresponding enzymes. After transformed into *Escherichia coli* and cultured on LB medium, the single colony was picked and were send to Sanger sequencing. Effective colony was further amplified in LB and Hipure Plasmid EF Maxi kit (Magen, China) and was used for plasmid extraction according to manufacturer's instructions.

Lentivirus generation

Dot1L shRNA (shDot1L) and the negative control vector (shCtrl) were purchased from Public Protein/Plasmid Library. To obtain the lentivirus, the recombinant plasmid shDot1L, or FoxO3a overexpression plasmid (FoxO3a OE) and packaging vector p Δ 8.2 and pVSVG were co-transfected into 293 T cells using transfection reagent lipofectamine 2000 (Invitrogen, USA). At 48 h and 72 h after transfection, the supernatant including lentivirus was collected and filtered by 0.45 μ m filter, concentrated by ultracentrifugation (25 000 rpm, 4 $^{\circ}$ C, 2 h; Beckham SW 28 rotor) and then re-suspended. Lentivirus carrying a negative control vector was prepared to check the efficacy of lentivirus particle for transfection and control experiments.

Small interfering RNA (siRNA) transfection

Dot1L siRNA (5'-GCAGAGGCUGUGACAAATT-3'; 5'-GCAGAAUCGUAUCCUCAATT-3'; 5'-CCAAAGUCCCUGAGAGCAATT-3'), FoxO3a siRNA (5'-CCCAGAUUCACGAGUGGAUTT-3'), and control siRNA were synthesized by Genepharma (Shanghai, China). Smad2/3 siRNA was purchased from Santa Cruz. Transfection of siRNA was performed when cells plated on 6-well plates reached a confluence of 60–80% via Lipofectamine RNAiMAX. siRNA and Lipofectamine RNAiMAX were respectively diluted to

proper concentration in Opti-MEM and then mixed and incubated at room temperature for 5 min, which was then added into the cells. After transfection for 24 h, the medium was replaced with serum-free DMEM medium and the efficiency of gene knockdown was examined by western blot at 72 h post-transfection.

Animal studies

Permission was obtained from Institutional Animal Care and Use Committee (IACUC), Fudan University, China. All animals and the experimental protocol were completely in accord with the Animal Welfare Act Guide for Use and Care of Laboratory Animals.

C57BL/6 mice (25–27 g) going through operation were randomly divided into three groups: the sham control group, myocardial infarction group (MI), Dot1L inhibitor EPZ5676 group (MI+EPZ5676). Mice in the latter two group were subjected to permanent ligation of the left ascending artery (LAD) to induce myocardial infarction. In brief, mice were anesthetized by isoflurane with the assistance of endotracheal intubation and rodent ventilator. After opening the chest cavity and subsequently removing the pericardium, the beating heart would be accessible. The descending branch of the LAD coronary artery was located and occluded with a 7–0 prolene suture. Upon ligation, the lower left part of the left ventricle will instantly turn pale, indicating a successful operation. EPZ5676 at doses of 20 mg/kg/day was administered to mice by intraperitoneal injection until the day before sacrifice.

A recombinant lentivirus vector carrying shDot1L was generated to explore the effect of Dot1L knockdown in vivo. After LAD ligation, the 150 μ L concentrated lentivirus carrying shDot1L or a negative control vector (shCtrl) was orthotopic injected around the edge of myocardial infarction area, respectively in shDot1L group and MI group. After 1 week, 150 μ L concentrated lentivirus was supplemented via tail vein respectively. Ultrasonic cardiogram and other analysis were performed on the surviving animals after 2 weeks.

Dot1L heterozygous knockout (Dot1L[±]) mice were generated on a C57BL/6 background under CRISPR/Cas system, for the sake of homozygous deletion of Dot1L led to embryonic lethality. Genotyping was performed using genomic DNA extracted from tails.

Echocardiography

Echocardiography was performed on spontaneously breathing mice as earlier described using VisualSonics Vevo 2100. Two-dimensional echocardiographic measurements were obtained. The ventricular dimensions (systolic and diastolic left ventricular internal diameter [LVIDs and LVIDd], as well as left ventricular end-diastolic and end-systolic volume [LVDD and LVSD]) were

calculated and determined. Both ejection fraction (EF) and fractional shortening (FS) were calculated separately for left ventricular pump function evaluation.

Histological evaluation and analysis of fibrosis

Mice were anesthetized by isoflurane and cervical dislocation after 14 days. The hearts were fixed in 4% Polyformaldehyde overnight and then were embedded in paraffin and stained with hematoxylin and eosin (H&E). To evaluate the histological change of fibrosis, the tissue sections were stained with Masson trichrome, according to the manufacturer's instructions, which could show collagen deposition in blue. The percentage of infarct area was defined by the ratio of fibrotic area with collagen deposition (blue) to the whole Masson's trichrome-stained section measured by Image J. For Sirius Red staining, sections were deparaffinized and rehydrated through gradient concentration of alcohols to distilled water. The sections were stained with Sirius red for 60 min at room temperature, followed by staining with hematoxylin for 10 min, according by the manufacturer's protocol. The collagen fibers including Col 1 and Col 3 were stained red, and muscle fibers as well as cytoplasm were stained yellow under light microscopy (Imager.M2, Zeiss, Germany).

Immunohistochemistry (IHC)

10% normal goat serum was used to block the sections, while diluted hydrogen peroxide (1:10 dilution of 3% hydrogen peroxide) to quench endogenous peroxidases. Then, the sections were incubated with primary mouse antibodies (Col 3 or Dot1L) overnight at 4 °C. Subsequently, immunohistochemistry was performed according to the kit protocol of the Biotin-Streptavidin Horseradish Peroxidase (HRP) detection system, using biotin-labeled goat anti-rabbit immunoglobulin IgG and streptavidin/HRP (ThermoFisher). All images were captured using a microscope (Axio Scope.A1, Carl Zeiss Imaging Systems).

Immunofluorescence

The cells seeded on glass coverslips going through corresponding treatment or tissue sections were fixed with 4% paraformaldehyde for 15 min. After permeabilization with 0.25% Triton X-100 for 10 min, the slides were blocked in 10% goat serum at least 30 min, and then incubated overnight with primary antibodies at 4 °C. Following incubation with appropriate secondary antibodies for 1.5 h at room temperature, the nuclei were stained with DAPI. All images were captured using a multi-channel fluorescence microscope (Zeiss).

Chromatin immunoprecipitation PCR (ChIP-PCR)

Under the guidance of the standard cross-linking ChIP protocol, the ChIP assays between H3K79me3 and FoxO3a gene promoter were performed. In Brief, cells digested by trypsin were crosslinked with 1% formaldehyde for 15 min at room temperature. DNA were sheared by sonication to get fragments of 300–1000 bp size, which were then immunoprecipitated with specific antibodies, with the same amount of non-specific IgG as control. The immunoprecipitated complex was rinsed, and DNA was extracted and purified. ChIP DNA was analyzed by qPCR on the FoxO3a gene promoter. The primer used for ChIP-PCR was as follows: forward: TAGCCGGCTGCTTTATCCTA; reverse: ACAGTCGTGCTTCGCTTTT.

Statistical analysis

Utilizing the GraphPad Prism 7.0 software for statistical analysis, data were reported as mean values \pm SD. Statistical significance between multiple groups were evaluated by one-way analysis of variance with Tukey's test for post hoc comparisons. $p < 0.05$ was considered to be statistically significant.

Abbreviations

Ang II: Angiotensin II; TGF- β 1: Transforming growth factor- β 1; CFs: Cardiac fibroblasts; NRCFs: Neonatal rat cardiac fibroblasts; Col 1: Collagen I; Col 3: Collagen III; CTGF: Connective tissue growth factor; Dot1L: Disruptor of telomeric silencing 1-like; ECM: Extracellular matrix; FMT: Fibroblast-to-myofibroblast transition; FN: Fibronectin; FoxO: Forkhead box O; LAD: Left ascending artery; MI: Myocardial infarction; MMPs: Matrix metalloproteinase; α -SMA: α -Smooth muscle actin.

Supplementary Information

The online version contains supplementary material available at <https://doi.org/10.1186/s13578-022-00877-5>.

Additional file 1: Fig. S1. Dot1L expression is mediated by p-Smad3 in Ang II-induced CFs. (A) p-Smad3 is upregulated in NRCFs treated with 2 μ mol/L Ang II for different times. Smad3 and its phosphorylation form were analyzed by western blot. (B) Smad2/3 knockdown attenuates Dot1L expression in Ang II treated NRCFs. Smad2/3 siRNA and control siRNA were transfected into NRCFs, followed by Ang II stimulation for 48 h. The protein expressions of Smad2/3, Dot1L, CTGF and Col 3 were analyzed by western blot. (C) Smad2/3 inhibition attenuates Dot1L expression in Ang II treated NRCFs. NRCFs were pretreated with Sis (0.5, 1, and 2.5 μ mol/L) for 4 h and then co-incubated with 2 μ mol/L Ang II for 48 h. Dot1L, Col 3, CTGF and MMP9 were analyzed by western blot. All data are presented as mean \pm SD. ANOVA, *** $p < 0.001$ versus Ctrl or Ctrl+siCtrl, ## $p < 0.01$, ### $p < 0.001$ versus Ang II or Ang II+ siCtrl, each acquired from three individual experiments

Acknowledgements

Not applicable.

Author contributions

J Xu, JH Wang and F Long performed the majority of experiments, analyzed the data, and drafted the paper. W Zhong, HB Su and ZH Su performed partial experiments and acquired the data. XH Liu designed the study, supervised the experiments, revised the manuscript and gave the final approval of the manuscript. All authors read and approved the final manuscript.

Funding

Project supported by Shanghai Municipal Science and Technology Major Project (Grant No. 2017SHZDZX01).

Availability of data and materials

The datasets used and/or analysed during the current study are available from the corresponding author on reasonable request.

Declarations**Ethics approval and consent to participate**

Permission was obtained from Institutional Animal Care and Use Committee (IACUC), Fudan University, China. All animals and the experimental protocol were completely in accord with the Animal Welfare Act Guide for Use and Care of Laboratory Animals.

Consent for publication

All the authors gave their approval for publication.

Competing interests

The authors declare no competing interest.

Received: 6 January 2022 Accepted: 9 August 2022

Published online: 19 August 2022

References

- Choudhury L, Mahrholdt H, Wagner A, Choi KM, Elliott MD, Klocke FJ, et al. Myocardial scarring in asymptomatic or mildly symptomatic patients with hypertrophic cardiomyopathy. *J Am Coll Cardiol*. 2002;40(12):2156–64.
- Wagner A, Schulz-Menger J, Dietz R, Friedrich MG. Long-term follow-up of patients with acute myocarditis by magnetic resonance imaging. *MAGMA*. 2003;16(1):17–20.
- Maceira AM, Joshi J, Prasad SK, Moon JC, Perugini E, Harding I, et al. Cardiovascular magnetic resonance in cardiac amyloidosis. *Circulation*. 2005;111(2):186–93.
- Gulati A, Jabbour A, Ismail TF, Guha K, Khwaja J, Raza S, et al. Association of fibrosis with mortality and sudden cardiac death in patients with nonischemic dilated cardiomyopathy. *JAMA*. 2013;309(9):896–908.
- Leong DP, Chakraborty A, Shipp N, Molaee P, Madsen PL, Joerg L, et al. Effects of myocardial fibrosis and ventricular dyssynchrony on response to therapy in new-presentation idiopathic dilated cardiomyopathy: insights from cardiovascular magnetic resonance and echocardiography. *Eur Heart J*. 2012;33(5):640–8.
- Fan D, Takawale A, Lee J, Kassiri Z. Cardiac fibroblasts, fibrosis and extracellular matrix remodeling in heart disease. *Fibrogenesis Tissue Repair*. 2012;5(1):15.
- Weber KT, Sun Y, Bhattacharya SK, Ahokas RA, Gerling IC. Myofibroblast-mediated mechanisms of pathological remodeling of the heart. *Nat Rev Cardiol*. 2013;10(1):15–26.
- Bollong MJ, Yang B, Vergani N, Beyer BA, Chin EN, Zambaldo C, et al. Small molecule-mediated inhibition of myofibroblast transdifferentiation for the treatment of fibrosis. *Proc Natl Acad Sci USA*. 2017;114(18):4679–84.
- Prabhu SD, Frangogiannis NG. The biological basis for cardiac repair after myocardial infarction: from inflammation to fibrosis. *Circ Res*. 2016;119(1):91–112.
- Hinz B, Phan SH, Thannickal VJ, Galli A, Bochaton-Piallat ML, Gabbiani G. The myofibroblast: one function, multiple origins. *Am J Pathol*. 2007;170(6):1807–16.
- Gabbiani G. The myofibroblast in wound healing and fibrocontractive diseases. *J Pathol*. 2003;200(4):500–3.
- Asano Y. Future treatments in systemic sclerosis. *J Dermatol*. 2010;37(1):54–70.
- Corso-Diaz X, Jaeger C, Chaitankar V, Swaroop A. Epigenetic control of gene regulation during development and disease: a view from the retina. *Prog Retin Eye Res*. 2018;65:1–27.
- Mitsiogianni M, Amery T, Franco R, Zoumpouris V, Pappa A, Panayiotidis MI. From chemo-prevention to epigenetic regulation: the role of isothiocyanates in skin cancer prevention. *Pharmacol Ther*. 2018;190:187–201.
- Stevenson TJ. Epigenetic regulation of biological rhythms: an evolutionary ancient molecular timer. *Trends Genet*. 2018;34(2):90–100.
- Delgado-Olguin P, Huang Y, Li X, Christodoulou D, Seidman CE, Seidman JG, et al. Epigenetic repression of cardiac progenitor gene expression by Ezh2 is required for postnatal cardiac homeostasis. *Nat Genet*. 2012;44(3):343–U158.
- Kang SH, Seok YM, Song MJ, Lee HA, Kurz T, Kim I. Histone deacetylase inhibition attenuates cardiac hypertrophy and fibrosis through acetylation of mineralocorticoid receptor in spontaneously hypertensive rats. *Mol Pharmacol*. 2015;87(5):782–91.
- Li YY, Wen H, Xi YX, Tanaka K, Wang HB, Peng DN, et al. AF9 YEATS domain links histone acetylation to DOT1L-mediated H3K79 methylation. *Cell*. 2014;159(3):558–71.
- Steger DJ, Lefterova MI, Ying L, Stonestrom AJ, Schupp M, Zhuo D, et al. DOT1L/KMT4 recruitment and H3K79 methylation are ubiquitously coupled with gene transcription in mammalian cells. *Mol Cell Biol*. 2008;28(8):2825–39.
- Steger DJ, Lefterova MI, Ying L, Stonestrom AJ, Schupp M, Zhuo D, et al. DOT1L/KMT4 recruitment and H3K79 methylation are ubiquitously coupled with gene transcription in mammalian cells. *Mol Cell Biol*. 2008;28(8):2825–39.
- Daigle SR, Olhava EJ, Therkelsen CA, Majer CR, Sneeringer CJ, Song J, et al. Selective killing of mixed lineage leukemia cells by a potent small-molecule DOT1L inhibitor. *Cancer Cell*. 2011;20(1):53–65.
- Mehta PK, Griendling KK. Angiotensin II cell signaling: physiological and pathological effects in the cardiovascular system. *Am J Physiol Cell Physiol*. 2007;292(1):C82–97.
- Zhang ZZ, Wang W, Jin HY, Chen X, Cheng YW, Xu YL, et al. Apelin is a negative regulator of angiotensin II-mediated adverse myocardial remodeling and dysfunction. *Hypertension*. 2017;70(6):1165–75.
- Worden EJ, Hoffmann NA, Hicks CW, Wolberger C. Mechanism of cross-talk between H2B ubiquitination and H3 methylation by Dot1L. *Cell*. 2019;176(6):1490.
- Schiano C, Benincasa G, Franzese M, Della Mura N, Pane K, Salvatore M, et al. Epigenetic-sensitive pathways in personalized therapy of major cardiovascular diseases. *Pharmacol Ther*. 2020;210: 107514.
- Nguyen AT, Xiao B, Neppel RL, Kallin EM, Li JA, Chen TP, et al. DOT1L regulates dystrophin expression and is critical for cardiac function. *Gene Dev*. 2011;25(3):263–74.
- Cattaneo P, Kunderfranco P, Greco C, Guffanti A, Stirparo GG, Rusconi F, et al. DOT1L-mediated H3K79me2 modification critically regulates gene expression during cardiomyocyte differentiation. *Cell Death Differ*. 2016;23(4):555–64.
- Farina FM, Serio S, Hall IF, Zani S, Cassanmagnago GA, Climent M, et al. The epigenetic enzyme DOT1L orchestrates vascular smooth muscle cell-monocyte crosstalk and protects against atherosclerosis via the NF-kappaB pathway. *Eur Heart J*. 2022. <https://doi.org/10.1093/eurheartj/ehac097>.
- Li F, Li L, Zhang J, Yang X, Liu Y. Histone methyltransferase DOT1L mediates the TGF-beta1/Smad3 signaling pathway through epigenetic modification of SYK in myocardial infarction. *Hum Cell*. 2022;35(1):98–110.
- Loffredo FS, Nikolova AP, Pancoast JR, Lee RT. Heart failure with preserved ejection fraction: molecular pathways of the aging myocardium. *Circ Res*. 2014;115(1):97–107.
- Kampaktis PN, Kokkinidis DG, Wong SC, Vavuranakis M, Skubas NJ, Devereux RB. The role and clinical implications of diastolic dysfunction in aortic stenosis. *Heart*. 2017;103(19):1481–7.
- Litwin SE, Katz SE, Morgan JP, Douglas PS. Serial echocardiographic assessment of left-ventricular geometry and function after large myocardial-infarction in the rat. *Circulation*. 1994;89(1):345–54.
- Burstein B, Libby E, Calderone A, Nattel S. Differential behaviors of atrial versus ventricular fibroblasts: a potential role for platelet-derived growth factor in atrial-ventricular remodeling differences. *Circulation*. 2008;117(13):1630–41.
- Chung CC, Kao YH, Yao CJ, Lin YK, Chen YJ. A comparison of left and right atrial fibroblasts reveals different collagen production activity and stress-induced mitogen-activated protein kinase signalling in rats. *Acta Physiol (Oxf)*. 2017;220(4):432–45.

35. Cohn JN, Ferrari R, Sharpe N. Remodeling IFC. Cardiac remodeling-concepts and clinical implications: a consensus paper from an international forum on cardiac remodeling. *J Am Coll Cardiol*. 2000;35(3):569–82.
36. van den Borne SWM, Diez J, Blankesteyn WM, Verjans J, Hofstra L, Narula J. Myocardial remodeling after infarction: the role of myofibroblasts. *Nat Rev Cardiol*. 2010;7(1):30–7.
37. Travers JG, Kamal FA, Robbins J, Yutzey KE, Blaxall BC. Cardiac fibrosis: the fibroblast awakens. *Circ Res*. 2016;118(6):1021–40.
38. MacLean J, Pasumarthi KBS. Signaling mechanisms regulating fibroblast activation, phenocconversion and fibrosis in the heart. *Indian J Biochem Biophys*. 2014;51(6):476–82.
39. Ronnebaum SM, Patterson C. The FoxO family in cardiac function and dysfunction. *Annu Rev Physiol*. 2010;72:81–94.
40. Tanaka H, Murakami Y, Ishii I, Nakata S. Involvement of a forkhead transcription factor, FOXO1a, in UV-induced changes of collagen metabolism. *J Investig Dermatol Symp Proc*. 2009;14(1):60–2.
41. Samarin J, Cicha I, Goppelt-Struebe M. Cell type-specific regulation of CCN2 protein expression by PI3K-AKT-FoxO signaling. *J Cell Commun Signal*. 2009;3(1):79–84.
42. Gomis RR, Alarcon C, He W, Wang QQ, Seoane J, Lash A, et al. A FoxO-Smad synexpression group in human keratinocytes. *Proc Natl Acad Sci USA*. 2006;103(34):12747–52.

Publisher's Note

Springer Nature remains neutral with regard to jurisdictional claims in published maps and institutional affiliations.

Ready to submit your research? Choose BMC and benefit from:

- fast, convenient online submission
- thorough peer review by experienced researchers in your field
- rapid publication on acceptance
- support for research data, including large and complex data types
- gold Open Access which fosters wider collaboration and increased citations
- maximum visibility for your research: over 100M website views per year

At BMC, research is always in progress.

Learn more biomedcentral.com/submissions

